Available online at www.sciencedirect.com
SCIENCE DIRECT®
Journal of Power Sources 144 (2005) 486–493
JOURNAL OF POWER SOURCES
www.elsevier.com/locate/jpowsour

Superior corrosion properties and reduced cost of lead–acid batteries using electroformed grids

Hans Warlimont*, Thomas Hofmann, Konrad Jobst

DSL Dresden Material-Innovation GmbH, Helmholtzstrasse 20, D-01069 Dresden, Germany

Received 14 October 2004; accepted 5 November 2004
Available online 29 January 2005

Abstract

A new technology for grid production by electroforming is found to improve grid properties and thus, to increase cycle-life, save costs, and increase the ecological efficiency of lead–acid batteries beyond the corresponding features of competing designs. The particular aspects of the superior corrosion behaviour of the new grids are addressed with respect to the effects of chemical and anodic processes, microstructure, corrosion-induced creep and grid growth, and adherence of the positive active-mass. Along with each of these factors of influence, the prospects for improving battery behaviour and lowering cost is also discussed. The properties achievable by using electroformed grids are presented in terms of experimental results from a comparison with the properties of conventional grids, and by modelling and simulation.

Keywords: Lead–acid battery; Microstructural effects; Corrosion; Grid growth; Electroforming; Positive active-mass

1. Introduction

The major aim of any development of new grid materials and grid structures for lead–acid batteries is to control the corrosion behaviour in order to enhance the performance and reduce the cost of the batteries. Grid corrosion is a key determinant of the functional properties and life of lead–acid batteries. Two effects dominate: (i) dissolution and disintegration of the grids through corrosive attack; (ii) corrosion-induced grid growth. Furthermore, the mode of grid corrosion and the properties of the oxides formed influence the interfacial resistance and the adherence of the positive active-mass. Therefore, the development of new grids aims at improvements through a melioration of corrosion-related effects. In the development of electroformed grids [1–3], we have studied their corrosion behaviour in comparison with that of conventional grids in order to elucidate any qualitative and quantitative improvements.

This study examines the factors that influence grid corrosion, namely, chemical and anodic processes, effects of microstructure, creep and grid growth, and adherence and contact resistance of the positive active-mass. The prospects for lower battery costs through the use of electroformed grids is also discussed.

2. Features and effects of grid corrosion

The corrosion of grid materials in lead–acid batteries leads to various effects that determine the functional properties, life and cost of the batteries. For example:

- *General corrosive dissolution*, mass loss and associated reduction in the cross-section of the grid structure (wires, spines) determine:
  - the duration of battery life;
  - the magnitude of plate resistance and ensuing battery power;
  - the gassing and ensuing water loss of the battery.

* Corresponding author. Tel.: +49 351 4659 400; fax: +49 351 4659 477.
E-mail address: warlimont@dsl-dresden.de (H. Warlimont).

0378-7753/$ – see front matter © 2004 Elsevier B.V. All rights reserved.
doi:10.1016/j.jpowsour.2004.11.052

- *Localised dissolution* by preferential attack along grain boundaries, as well as along other boundaries such as those of precipitates, inclusions and weld interfaces, determines:
  - the duration of battery life as dependent on grid disintegration;
  - the magnitude of plate resistance and ensuing battery power.
- *Oxide formation* determines:
  - the corrosion-induced grid growth due to the volume difference between metal and oxide and build-up of stresses and strains, which result in shedding of the active mass and, there by, premature capacity loss;
  - the contact resistance between the grid and the active mass and its effect on battery power.

The mechanism and rate of corrosion are influenced by:

- the composition, microstructure and properties of the grid material;
- the corrosion conditions, as dictated by the type of battery operation;
- grid, plate and battery design.

This list of causes and effects shows that the development of new grids is a task of simultaneous engineering. This has essentially been achieved through the development of electroformed grids that have superior corrosion properties compared with present-day grids, as well as high economic and ecological efficiency [4].

3. Chemical and anodic corrosion

3.1. Corrosion testing

The rate of corrosion is generally defined by the rate of mass loss per unit area of a planar interface, i.e.,

$$v_{T,E,j} = \frac{\mathrm{d}m_\mathrm{M}}{\mathrm{d}t\,A} = \frac{\Delta m_\mathrm{M}}{\Delta t\,A} = \frac{\text{weight loss}}{\text{time} \times \text{specimen surface}} \quad (1)$$

where Δm_M is the mass of metal or alloy dissolved during the test time Δt and A is the area exposed to corrosion. In chemical corrosion, it is assumed that the temperature T and the area A are constant. In electrochemical corrosion, the applied potential E (in potentiostatic testing) or the current density j (in galvanostatic or constant-current testing) is also assumed to remain constant. Obviously then, the simple relation (1) does not hold for all grid corrosion tests, since the geometry changes with time such that A and j become time-dependent. Furthermore, no rate-determining effect by oxide formation is included in relation (1). Semiconducting oxide is formed and this may determine the rate of corrosion increasingly as its formation proceeds to the extent that the mechanism and kinetics of oxide formation dominate the reaction kinetics more than the chemical or anodic process of grid corrosion. If the rate of corrosion of grids is determined from measurements of the mass loss of pasted grids, the properties and the geometry of the active mass must be taken into account. In general, the active mass decreases the rate of corrosion, but in detail the rate is time-dependent as corrosion proceeds [5].

This brief discussion shows that most results obtained from investigations of the rates of corrosion of different grids cannot be compared quantitatively to a reasonably high degree of accuracy because they depend not only on the differences in experimental conditions, but also on the differences in specimen design and dimensions. For grid specimens of identical design and size, only an 'effective' rate of corrosion can be obtained by measuring the mass loss $\Delta m_{\mathrm{M,eff}}$. This procedure can, however, serve to compare different grid materials to assess the effects of differences in chemical composition and microstructure.

3.2. Corrosion data

Numerous studies of the corrosion of planar samples have been performed to quantify the basic chemical corrosion behaviour of lead and lead alloys, particularly in sulfuric acid [6]. For chemical corrosion, Hofmann [7] has summarized that at 20 °C in a 70% aqueous solution of H_2SO_4, the rate of corrosion (v) varies from 0.7 to 2.9 mg cm^{-2} (10 d)$^{-1}$ when going from high purity Pb to Pb–0.1 wt.% Cd in a series of about 40 different grades of Pb and dilute Pb alloys. This is equivalent to a reduction in thickness from 0.6 to 2.6 μm in 10 days.[1] Chemical corrosion of Pb–Sn alloys as a function of Sn content and acid concentration in boiling H_2SO_4 [6] has been shown to exhibit a maximum at about 0.3 wt.% Sn. At higher Sn contents, the rate of corrosion decreases with increasing Sn content. Copper in excess of 0.01 wt.% drastically decreases the rate of chemical corrosion of lead in boiling H_2SO_4 (70% aqueous solution) from about 2500 μm (10 d)$^{-1}$ to ∼110 μm (10 d)$^{-1}$ [8].

Systematic measurements of anodic corrosion are of particular relevance for the development of improved grid materials if they show quantitavely the effects of Ca and Sn on the effective rate of corrosion of plate specimens of Pb–Ca–Sn. The results shown in Fig. 1 [9] were obtained by galvanostatic polarization at 22 °C and at a current density $j = 0.84$ mA cm^{-2}. The data shown in Fig. 2[2] were obtained at 50 °C and at $j = 8.6$ mA cm^{-2}. The data in Figs. 1 and 2 indicate quantitatively that Ca increases, and Sn decreases, the rate of corrosion under both test conditions significantly. It is interesting to note that the effect of Sn concentration on the rate of corrosion decreases with decreasing Ca content. Other systematic corrosion measurements on Pb–Ca–Sn grids with varying Ca and Sn contents at 40 [5] and 50 °C [10] have led to corresponding results. Silver additions in the range of 0.02–0.07 wt.% Ag decrease the rate of corrosion, but increase the oxygen evolution [11].

[1] Wherever it appears reasonable, we have recalculated and normalized various data from the literature to a corrosion time of 10 days, i.e., (10 d)$^{-1}$, in order to facilitate comparisons.

[2] Data provided by a major battery manufacturer.

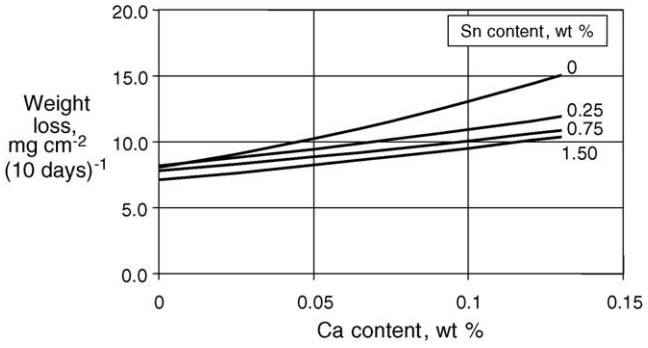

Fig. 1. Weight loss by corrosion of Pb–Ca–Sn alloys at room temperature (≈22 °C). Cast plate samples test parameters: $j = 0.84\,\text{mA cm}^{-2}$, $t = 45$ days, $H_2SO_4 = 1.25\,\text{g cm}^{-3}$. Data of [9], converted to weight loss in 10 days, re-plotted, and extrapolated to 0 wt.% Ca.

The designation j_i, the initial current density, should be used for all 'galvanostatic' tests of grids in order to recognize that these grid tests are not galvanostatic at all. The current density (j_i) relates only to the initial grid surface. In actual tests, the current is kept constant. Since the corrosive dissolution of the grid leads to a continuous decrease of the grid surface, the current density increases continuously during the test and the results become dependent on the initial cross-section and shape of the grid wires. In this paper, the designation j_i is used deliberately for all 'galvanostatic' tests. A simple geometric consideration shows, for example that removal of a 85-μm layer by corrosion leads to a 20% increase in current density if the initial wire cross-section is 1 mm × 2 mm, and to a 40% increase in current density if it is 0.6 mm × 1.2 mm. This means that a 'galvanostatic' grid corrosion test is invariably a self-accelerating test and is dependent on the individual grid geometry. Thus, test results obtained from grids under nominally identical constant current conditions are not comparable.

The rate of grid corrosion is decreased in the presence of positive active-mass [12,13]. Detailed measurements have shown [13] that the rate of corrosion of bare grids decreases with time of exposure due to oxide formation, and then remains constant. A linear dependence of corrosion on time sets in when the oxide layer begins to form cracks and disintegrates due to the stresses built up after a critical thickness has been attained. At this stage, the rates of oxide formation and oxide disintegration reach a steady state. The rate of corrosion of grids covered with active mass is decreased by at least a factor of two compared with that of bare grids. It is also observed that this 'protection factor' depends not only on the composition and thickness of the active mass, but also on the rate of corrosion of the alloy.

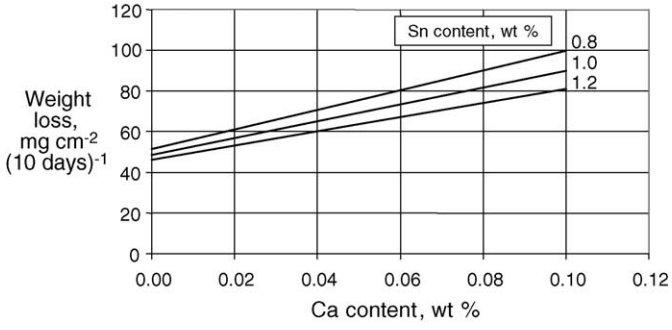

Fig. 2. Weight loss by corrosion of Pb–Ca–Sn alloys at 50 °C. Cast plate samples test parameters: $j = 8.6\,\text{mA cm}^{-2}$, $t = 14$ days, $D\,(H_2SO_4) = 1.28\,\text{g cm}^{-3}$. Original data converted to weight loss in 10 days, re-plotted, and extrapolated to 0 wt.% Ca.

3.3. Anodic corrosion of electroformed grids

Previous studies have shown that pure binary Pb–Sn alloys provide the most stable chemical composition under conditions of battery operation. Therefore, a binary Pb–Sn coating is used as the major coating layer of electroformed grids. The results at elevated temperature, shown in Fig. 2, are particularly relevant for this choice because testing at higher temperatures is in accordance with the temperature regimes that are characteristic of modern cars. Taken at face value, the data show that the amount of corrosion is reduced by about 30% in going from about 0.07 wt.% Ca, which is representative for present grid alloys, to 0 wt.% Ca. This can be translated into either keeping the same grid thickness and increasing the battery life by approximately 30%, or decreasing the grid thickness by 30% – and saving the Pb cost accordingly – while keeping the average battery life the same as before.

Since present Pb–Ca–Sn based grid materials contain Ca, Al, and Ag as alloying additions to provide hardenability and increase corrosion resistance, these alloy components add significantly to the material cost through the alloy premium. All three components are unnecessary in the electroformed grids. Thus, the alloy premium for electroformed grids is significantly lower; this lowers their raw material cost still further.

4. Effects of microstructure on corrosive attack

4.1. Comparison of different grid structures

A decisive difference in corrosive attack arises from the differences in grid microstructure that arise from the use of varions production processes. The primary factors of influence are: grain size, grain shape, and orientation of grain boundaries with respect to the corroding interface. Since grain boundaries are lattice defects of higher energy than the grains themselves, they will invariably be local paths of higher rates of attack. Their energy depends strongly on the crystallographic type of each individual boundary in the sense that the higher is the structural disorder, the higher is the energy and, vice versa, and the rate of corrosive attack varies accordingly [14]. The instability to corrosion may be increased by grain boundary segregation if the segregated component is enhancing corrosion. Similarly, the precipitates that form

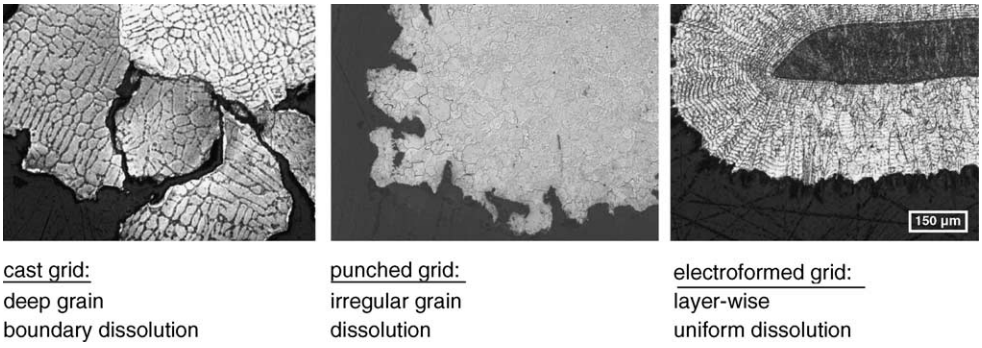

Fig. 3. Microstructures of grids produced by different manufacturing processes and subjected to a bare-grid corrosion test at 75 °C at $j_i = 6\,mA\,cm^{-2}$, D (H_2SO_4) = 1.28 g cm^{-3}.

along the grain boundaries increase the local rate of attack if they contain components prone to corrosion. The reverse is true, if segregated atoms or precipitated phases increase the stability against corrosion.

The characteristic and decisive differences in corrosion behaviour between the grids made by the major processes of present grid production are illustrated by the micrographs in Fig. 3. All specimens were subjected to bare-grid corrosion tests under identical conditions, namely: 75 °C, 6 mA cm^{-2}, 10 days, D (H_2SO_4) = 1.28 g cm^{-3}. It is immediately obvious that the cast grids are most prone to grain-boundary attack. The depth of penetration along the grain boundaries essentially determines the mechanical instability of the grid and leads to catastrophic failure by early wire breakage [5], even if the general weight loss is low. Grain-boundary attack is reduced in Ag-alloyed cast grids but at the expense of a higher alloy premium.

4.2. Mode of attack of electroformed grids

The layer-like deposition of the grid structure in the coating stage of the dispersion strengthened lead (DSL) electroforming process yields a variation in Sn content between adjacent layers. Typically, this variation may be of the order of ±0.2 wt.% Sn. This leads to a layer-wise, almost uniform, dissolution of the grid material as shown in Fig. 4. Due to this uniform dissolution layer by layer, the corrosion attack along grain boundaries is limited to the actual corroding layer and is impeded at each Sn-rich layer so that deep crevice formation is inhibited. No exfoiliation occurs with electroformed grids because the grain boundaries are normal to the free surface and the layer interfaces of varying Sn concentration do not interrupt the coherency of the crystal lattice, i.e., they are not grain boundaries. The integrity of electroformed grids is maintained for much longer than for grids made by conventional processes, in particular book-mould casting, which lead to microstructures that are prone to deep grain-boundary corrosion. The electroformed grids remain ductile practically until the end of battery life. The technical result of this unique behaviour was borne out upon tear-down analysis of batteries subjected to the corrosion test according to the VW 750 73 battery test standard. It was found that the grids, which had lost about half of their thickness, were still fully ductile, i.e., they did not show any wire breaks. In plate form, electroformed grids have also passed the SAE-J240 test that applies 1500 cycles at 75 °C.

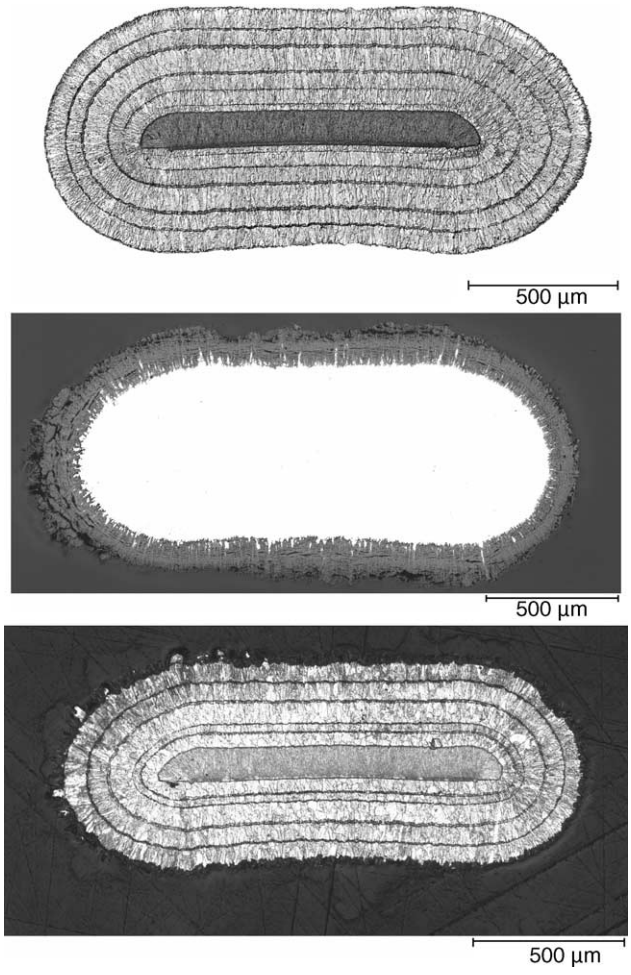

Fig. 4. Cross-section of a wire of a DSL grid before and after corrosion testing. Layer-like, uniform corrosive dissolution. Top: cross-section of grid as formed; centre: after corrosion, unetched, showing oxide layer; bottom: after corrosion, etched, oxide layer removed.

5. Grid growth

5.1. Driving forces and modes of growth

The grid growth of bare grids is caused by the oxidation process because the specific volume of the oxide β-PbO_2 is 22% higher than that of the Pb from which it is formed [15]. During plate formation and battery charging, the volume increase of the oxide formed on the grid wires causes a tensile force. The resistance to this force is given by the creep strength of the grid alloy times the effective cross-section of the grid wires. During battery operation, the positive active-mass adds to this effect. While β-PbO_2 has a specific volume of 0.108 $cm^3\,g^{-1}$, $PbSO_4$ has a specific volume of 0.159 $cm^3\,g^{-1}$. Even though the positive active mass is porous, part of the volume difference will build up tensile stress on the grid wires. The charging and discharging cycles exert a concomitant cyclic stress reversal on the grid wires and lead to the accumulate effect of grid growth. In addition, the oxide formation along the grain boundaries of cast grids enhances the growth strain because it is essentially irreversible. Thus, the microstructural features that result from the process of grid production play a significant role in grid growth.

Grid growth can be observed in bare-grid corrosion as well as in plate corrosion tests. A typical example of grid growth data and some plate growth data obtained from Pb–Ca–Sn–Al alloy grids for industrial batteries has been reported by Giess [17]. A summary of the results is given in Fig. 5. Two dominating factors of influence on the magnitude of grid growth may be recognized, namely, the grid thickness and the strength of the grid alloy. In addition, there are significant differences in microstructure and concomitant observations of differences in the amount and the penetration of oxide layers along the grain boundaries, which can be correlated to the extent of grid growth. Extensive growth data have also been published by Fouache et al. [16] for the effects of Ca, Sn, Ag, the process of grid making (rolled expanded versus gravity cast), the state of heat treatment, and the time or schedule of exposure. The results correspond essentially to those quoted above.

5.2. Growth of electroformed grids

Typical growth data for experimental DSL electroformed grids are shown in Fig. 6. If the grid core is made of soft Pb–Sn only, the growth is comparatively high and is accelerated with time of exposure. If the grid core is dispersion hardened, however, the grid growth is decreased significantly. The composite structure of the DSL grids permits control of the rate of growth by adjusting the strength and the fractional cross-section of the grid core.

Numerous parameters are influential in grid growth and the geometric variability of grid structures does not permit reliable transfer of data obtained from model experiments to different grids in technical use. Therefore, it was decided to carryout extensive calculations based on modelling and simulation of the growth process. The prime aim is to understand qualitatively and semi-quantitatively how the main factors of influence affect the amount of growth strain. The results from a simple model for uniform grid material have been reported previously [3]. In those simulations, it was revealed for massive grid materials how variations of the width of the grid wires, which is proportional to their cross-section, and of the yield stress of the material affect the magnitude of grid growth.

In subsequent work, the growth strain of a composite grid wire, which is representative of the composite structure of the DSL grids, has been modelled and simulated. The aim of this calculation is to assess the compound effects of different levels of yield stress and thickness of the core with different total thicknesses of the grid wire. The cross-section of the wire model consisting of the core and the outer coating layer of the grid wire is shown in Fig. 7(a). The additional surface layer permits simulation of the expanding force of the oxide and positive active-mass and the growth strains that they cause. The magnitude of the total strain vector $\boldsymbol{\varepsilon}_{tot} = \boldsymbol{\varepsilon}_x + \boldsymbol{\varepsilon}_y$ is given in Fig. 7(b). The particular strain distribution results

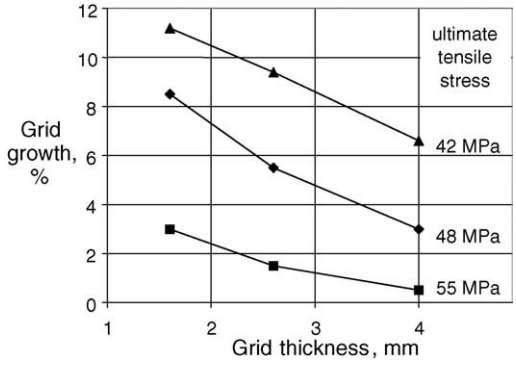

Fig. 5. Test results of corrosion-induced grid growth for Pb–Ca–Sn–Al alloys of different composition and thickness in cast industrial battery grids [17].

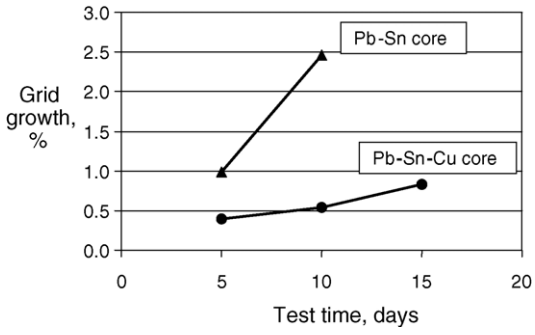

Fig. 6. Corrosion-induced bare-grid growth observed by testing experimental electroformed DSL composite grids of different composition containing a soft (Pb–1 wt.% Sn) and a hard (Pb–1 wt.% Sn–0.3 wt.% Cu) core, respectively. Test conditions: 75 °C, $j_i = 6\,mA\,cm^{-2}$, $D\,(H_2SO_4) = 1.28\,g\,cm^{-3}$.

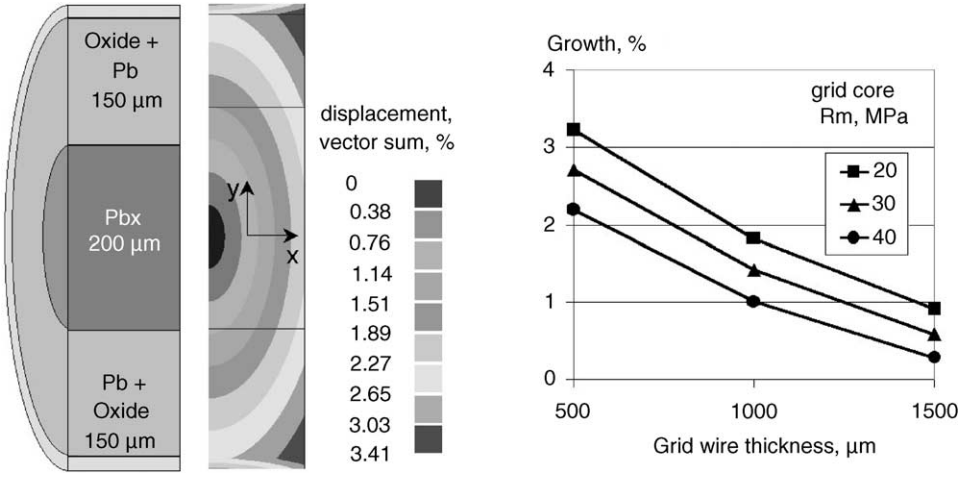

Fig. 7. Simulation of corrosion-induced grid growth based on modelling of a composite grid wire. Left: model structure, composite layers; centre: strain distribution due to tensile stress built up in outer oxide layer; right: selected strain data in *x*-direction that indicate the dependence of grid growth on core strength and grid thickness.

from the differences in mechanical properties between the core and the coating, and from the stress and different elastic moduli assumed for the oxide layer. Some characteristic results of the simulation are summarized in Fig. 7(c). This is a plot of the strain component ε_x, which is equivalent to the overall growth strain, as a function of grid thickness, core diameter, and yield strength of the core material. The diagram shows that a given specification of maximum permissible grid growth can be met by different combinations of grid thickness, core thickness, and core strength as design parameters. The core strength can be adjusted by different mechanisms that have been established during the developmental work.

Acceptable amounts of grid growth are specified in various statements and standards. According to [17], magnitudes of growth that are adequate for long-life value-regulated lead–acid (VRLA) batteries are 3–6% in 54 weeks at 60 °C. According to VW standard 750 73, maximum growth in the direction of grid height must remain below 2 mm.

In conclusion, it can be stated that electroformed grids can be produced to conform to any specified growth limits by utilizing the variability of the parameters that are available in the manufacturing process of the electroformed composite grid, i.e., strength of the core, thickness of the core, and thickness of the grid.

6. Corrosion-assisted increase of adherence of active mass and decrease of contact resistance

The initial formation of a solid-state bond between the grid surface and the positive active mass, the subsequent process of oxide formation, and the properties of the interfacial oxide layer are decisive for the adherence of the active mass and for a high conductivity across the interface. There are three factors of influence that may be optimized to achieve optimum properties at the interface, i.e.,

- favourable corrosive behaviour of the grid surface for the formation of the initial oxide layer;
- sufficient Sn concentration to prevent the formation of a passivating PbO layer with a high electrical resistance on deep discharge;
- controlled roughness to provide a high interfacial area and favourable conditions for contact at the interface between the metal and the positive active-mass.

6.1. Corrosive behaviour of grid surface

In battery manufacturing, the process of plate formation in an electrolyte of high pH is associated with the initial formation of a passivating interfacial layer between the grid surface and the active mass. This layer consists of β-PbO_2, which persists as long as acidic conditions prevail. The oxide is formed on the surface grains and preferentially along grain boundaries. Therefore, if grain boundaries near the grid surface are provided at a high density per unit area and are oriented predominantly normal to the surface, they serve optimally as short local paths of oxide formation and result in an interlocking structure between the metal and the oxide.

6.2. Favourable microstructure at surface of electroformed grids

A favourable microstructure is ideally realized by galvanic deposition if the conditions are chosen in such a way as to favour columnar crystal growth. Such growth usually occurs at a comparatively high current density. The surface of an electroformed DSL grid which exhibits exactly this kind of ideal microstructure is shown in Fig. 4. The subsequent interlocking microstructure with the β-PbO_2 phase has grown partly into the material along the grain boundaries. This is revealed most clearly by the micrograph shown in the centre of Fig. 4.

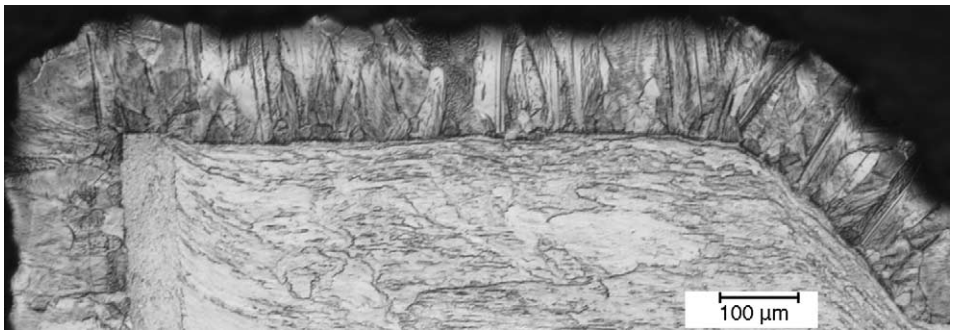

Fig. 8. Galvanic coating of a punched grid. The microstructure shows cross-section of a grid wire. The coating reveals columnar grain growth. The Sn content was chosen to be higher than that of the substrate grid.

6.3. *Sufficiently high tin content*

The effect of additions of Sn to the grid alloy to decrease the rate of corrosion and the thickness of the passivating α-PbO (tetragonal PbO) layer formed upon deep cycling has been studied by Giess [18]. It was established that Sn additions between 0.2 and 0.4 wt.% decreased the polarization and increased the charge-acceptance significantly. Simon et al. [19,20] analysed the effect of Sn additions further. The electronic conductivity of α-PbO in a series of Pb–Sn alloys was studied by determining polarization currents and X-ray photoelectron spectroscopy (XPS) spectra of the oxide layers formed in a basic solution. It was found that the passive layer of PbO shows no electron transfer if the alloy contains less than 0.8 wt.% Sn. Above this concentration, the conductivity of the passivating layer increases sharply. It was also established that as the alloy content was raised from 0.5 to 2.5 wt.% Sn, the Sn concentration of the oxide layer rose from 3 to 44 wt.% Sn. Moreover, in accordance with the earlier investigations [18], it was found [10,20] that the thickness of the PbO layer is decreased with increasing Sn content, which contributes to the lowering of its resistance. By metallographic analysis, it was found that at tin levels between 1 and 1.5 wt.%, at which the alloy is a homogeneous solid solution, the highly conducting SnO_2 phase is precipitated along the PbO grain boundaries. At tin contents greater than 1.5 wt.%, the alloy is two-phased and a very thin SnO_2 oxide layer is formed directly at the grid surface [21].

6.4. *Higher Sn content at free surface of electroformed grids*

In producing grids by the electrodeposition process, the inherent use of a sequence of galvanic baths permits the application of a final layer of increased Sn-concentration without major modification of the equipment and at low cost. For example, a final surface coating of 10 μm thickness and 1.5–2 wt.% Sn may be applied. By virtue of this feature, the DSL process provides a possibility to optimize battery behaviour in terms of charge-acceptance of the plates by controlling the formation of a PbO layer with a low thickness and a high conductivity upon deep cycling. This would provide low polarization upon charging and a significant reduction in premature capacity loss.

6.5. *Controlled surface roughness of electroformed grids*

In contrast to all other grid-making processes, galvanic deposition according to the DSL process allows control of the surface roughness reproducibly within wide limits. This is simply achieved by a suitable combination of bath additives and control of the current density applied in the final stage of grid deposition. For example, roughness curves have shown [3] that the average roughness value $R_a \approx 4$ μm of a 'natural', fairly smooth deposit can be increased to $R_a \approx 40$ μm. Obviously, such a high increase is associated with a concomitant increase in interfacial area and, thus, in a potentially higher adherence of the positive active-mass, which contributes further to a reduction in premature capacity loss.

6.6. *Galvanic coating of expanded and punched grids*

A galvanic surface layer can also be applied to grids made by rolled and expanded, or rolled and punched, strip material. Such a coating process, which can be integrated directly in a plate-making line, provides the same improved surface properties as for fully electroformed grids. An example of a favourable surface layer on a punched grid is shown in Fig. 8.

7. Conclusions

The innovative process of electroforming of battery grids permits, for the first time, the production of grids as composite materials that exhibit corrosion properties superior to those found with all present processes for grid-making. Accordingly, these novel grids provide superior battery properties and the unique prospect of lower battery costs.

In detail, the advantages in corrosive behaviour analyzed in this paper lead to the following conclusions:

(i) The major fraction of the grid cross-section can be made of pure Pb–Sn and this lowers the corrosion rate by

about 25–30% compared with Pb–Ca–Sn grids. This can be exploited by saving about 25–30% of grid thickness and, thus, saves lead cost without decreasing battery life; moreover, the alloy premium for Ca and Ag can be saved.

(ii) The microstructure of the grid is a multilayer composite of periodically varying Sn content. Therefore, the corrosive attack occurs layer by layer without deep grain-boundary attack. Consequently, the grid remains intact and flexible throughout the life of the battery. There is no catastrophic premature grid failure by deep crevice formation.

(iii) The corrosion-induced grid growth of electroformed grids can be controlled easily and can be limited to a specified maximum by producing a grid core of sufficient strength in the first stage of the electroforming process. The yield and creep strength of the core material can be adjusted effectively by dispersion hardening.

(iv) The outer grid surface can be alloyed and structured specifically without an extra process step. Thus, paste adherence can be increased to extend cycle-life. Concurrently, the formation of a highly conducting, Sn-rich oxide layer by corrosion can be induced by a higher Sn content (>1.5 wt.% Sn) in the outmost surface layer. This improves charge-acceptance upon deep discharge significantly.

The technology of galvanic coating to attain the abovementioned surface properties can also be applied to coat grids of the conventional expanded or punched type.

In summary, it can be concluded that electroformed grids improve battery behaviour while saving cost and increasing both economic and ecological efficiency.

Acknowledgements

This work was funded in part by the Federal Ministry of Economy and Labour of the Federal Republic of Germany through its FUTOUR programme and by the State Ministry of Economy of the Free State of Saxony through its programme for the promotion of industrial research and development.

References

[1] G. Barkleit, A. Grahl, M. Maccagni, M. Olper, P. Scharf, R. Wagner, H. Warlimont, J. Power Sources 78 (1999) 73–78.
[2] German Patent 4,404,817, US Patent 5,672,181, further patents granted and pending.
[3] H. Warlimont, T. Hofmann, J. Power Sources 133 (2004) 14–24.
[4] H. Warlimont, Mater. Trans. 44 (2003) 1232–1236.
[5] C.S. Lakshmi, J.E. Manders, D.M. Rice, J. Power Sources 73 (1998) 23–29.
[6] E. Wendler-Kalsch, H. Gräfen, Korrosionsschadenskunde, Springer-Verlag, Berlin, Germany, 1998.
[7] W. Hofmann, Lead and Lead Alloys, Springer-Verlag, Berlin/Heidelberg/NY, USA, 1970.
[8] E. Pelzl, Metallurgy 21 (1967) 826.
[9] R.D. Prengaman, J. Power Sources 67 (1997) 267–278.
[10] L. Albert, A. Chabrol, L. Torcheux, Ph. Steyer, J.P. Hilger, J. Power Sources 67 (1997) 257–265.
[11] S. Zhong, J. Wang, H.K. Liu, S.X. Dou, M. Skyllas-Kazacos, J. Appl. Electrochem. 290 (1999) 1–6.
[12] S. Feliu, L. Galan, J.A. Gonzalez, Werkstoffe und Korrosion 23 (1972) 554–561.
[13] J. Garche, J. Power Sources 53 (1995) 85–92.
[14] E.M. Lehockey, G. Palumbo, P. Lin, A. Brennenstuhl, Metall. Mater. Trans. A Phys. Metall. Mater. Sci. 29 (1998) 387–396.
[15] Jürgen O. Besenhard (Ed.), Handbook of Battery Materials, Wiley–VCH Weinheim, NY, USA, 1999.
[16] S. Fouache, A. Chabrol, G. Fossati, M. Bassini, M.J. Sainz, L. Atkins, J. Power Sources 78 (1999) 12–22.
[17] H. Giess, J. Power Sources 53 (1995) 31–43.
[18] H. Giess, Proceeding Symposium on Advances in Lead-Acid Batteries, vol. 84.14, Electrochemical Society, Pennington NJ, USA, 1984, pp. 241–251.
[19] P. Simon, N. Bui, F. Dabosi, J. Power Sources 50 (1994) 141–152.
[20] P. Simon, N. Bui, F. Dabosi, G. Chatainier, M. Provincial, J. Power Sources 52 (1994) 31–39.
[21] E. Rocca, J. Steinmetz, Electrochim. Acta 44 (1999) 4611–4618.